

Macrocyclic Hydroperoxocobalt(III) Complex: Photochemistry, Spectroscopy, and Crystal Structure

Ilia A. Guzei[†] and Andreja Bakac*

Ames Laboratory, Iowa State University, Ames, Iowa 50011

Received December 8, 2000

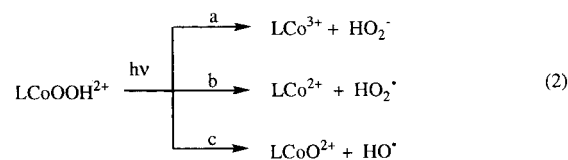
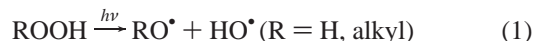
The hydroperoxocobalt complex $[L^2(\text{CH}_3\text{CN})\text{CoOOH}](\text{ClO}_4)_2 \cdot \text{CH}_3\text{CN}$ ($L^2 = \text{meso-5,7,7,12,14,14-Me}_6\text{-[14]aneN}_4$) crystallizes with discrete anions, cations, and solvate acetonitrile molecules in the lattice. The complex crystallizes in the monoclinic space group $P2_1/n$, $a = 10.4230(5) \text{ \AA}$, $b = 16.1561(8) \text{ \AA}$, $c = 17.4676(9) \text{ \AA}$, $\beta = 92.267(1)^\circ$, $V = 2939.2(3) \text{ \AA}^3$, $Z = 4$. The O–O bond length is $1.397(4) \text{ \AA}$, and the O(2)–O(1)–Co angle spans 117.7° . The O–O stretch in the infrared spectrum appears at 815 cm^{-1} . The 355- and 266-nm photolysis of acidic aqueous solutions of $L^2(\text{H}_2\text{O})\text{CoOOH}^{2+}$ results in homolytic splitting of the Co–O bond and yields $L^2\text{Co}(\text{H}_2\text{O})_2^{2+}$ and $\text{HO}_2^\bullet/\text{O}_2^{\bullet-}$ as the only products. The two fragments were scavenged selectively in separate experiments with O_2 and $\text{C}(\text{NO}_2)_4$. There is no evidence for photochemical O–O bond homolysis, presumably because the appropriate optical transition is masked by the HO_2 -to-Co LMCT transition.

Introduction

Metal hydroperoxo complexes are important intermediates in enzymatic and catalytic oxidations with molecular oxygen and hydrogen peroxide. For example, the active form of antitumor drug bleomycin contains an Fe–OOH group, as shown by electrospray mass spectrometry.¹ In cytochrome P 450-catalyzed oxidations, hydroperoxo iron species play a dual role as both precursors to the active iron-oxo form (“oxene”)² and active oxidants.³ Hydroperoxo complexes of several other metals and ligand systems have been prepared in the laboratory and characterized spectroscopically and chemically.^{4–9} The number of crystal structure determinations of such metal η^1 -OOH species remains, however, quite limited.^{9–15}

A complex believed to be $L^2(\text{H}_2\text{O})\text{CoOOH}^{2+}$ ($L^2 = \text{meso-5,7,7,12,14,14-Me}_6\text{-[14]aneN}_4$) was prepared previously in our laboratory.¹⁶ The hydroperoxo structure for this and the related complex $L^1(\text{H}_2\text{O})\text{CoOOH}^{2+}$ ($L^1 = [14]\text{aneN}_4$)^{17,18} was inferred on the basis of the preparative method used and the chemical reactivity of the two complexes. These compounds were prepared by controlled chemical^{16,17} or electrochemical¹⁸ reduction of the superoxo precursors $L(\text{H}_2\text{O})\text{CoOO}^{2+}$ ($L = L^1$ and L^2) and both exhibited Fenton-type chemistry in reactions with reducing metal complexes.¹⁶ The results are fully consistent with a hydroperoxo structure, although an η^2 -peroxo complex could not be completely ruled out. We have now determined the crystal structure of the CoL^2 complex to resolve the structural issues.

The second aspect of this work deals with the photochemistry of $L(\text{H}_2\text{O})\text{CoOOH}^{2+}$ complexes. Unlike the straightforward photochemistry of hydrogen peroxide and alkyl hydroperoxides, both of which undergo clean O–O bond cleavage upon irradiation with UV light, eq 1, metal hydroperoxides would seem to offer several possibilities: hydrolysis of metal–hydroperoxide bond, homolysis of metal–hydroperoxide bond, and homolysis of the O–O bond, as shown in eq 2.



The photochemistry of η^1 metal hydroperoxides is largely unexplored, but the peroxo complexes have received some

* To whom correspondence should be addressed. E-mail: Bakac@ameslab.gov.

[†] Current address: Department of Chemistry, University of Wisconsin, Madison, WI 53706.

- (1) Sam, J. W.; Tang, X.-J.; Peisach, J. *J. Am. Chem. Soc.* **1994**, *116*, 5250–5256.
- (2) Lippard, S. J.; Berg, J. M. In *Principles of Bioinorganic Chemistry*; University Science Books: Mill Valley, 1994; Chapter 11.
- (3) Newcomb, M.; Toy, P. H. *Acc. Chem. Res.* **2000**, *33*, 449–455.
- (4) Wang, W.-D.; Bakac, A.; Espenson, J. H. *Inorg. Chem.* **1993**, *32*, 2005–2009.
- (5) Ho, R. Y. N.; Roelfes, G.; Hermant, R.; Hage, R.; Feringa, B. L.; Que, L., Jr. *Chem. Commun.* **1999**, 2161–2162.
- (6) Roelfes, G.; Lubben, M.; Chen, K.; Ho, R. Y. N.; Meetsma, A.; Genseberger, S.; Hermant, R. M.; Hage, R.; Mandal, S. K.; Young, V. G., Jr.; Zang, Y.; Kooijman, H.; Spek, A. L.; Que, L., Jr.; Feringa, B. L. *Inorg. Chem.* **1999**, *38*, 1929–1936.
- (7) Mirza, S. A.; Bocquet, B.; Robyr, C.; Thomi, S.; Williams, A. F. *Inorg. Chem.* **1996**, *35*, 1332–1337.
- (8) Wu, W.; Vanderwall, D. E.; Lui, S. M.; Tang, X.-J.; Turner, C. J.; Kozarich, J. W.; Stubbe, J. *J. Am. Chem. Soc.* **1996**, *118*, 1268–1280.
- (9) Wick, D. D.; Goldberg, K. I. *J. Am. Chem. Soc.* **1999**, *121*, 11900–11901.
- (10) Wada, A.; Harata, M.; Hasegawa, K.; Jitsukawa, K.; Masuda, H.; Mukai, M.; Kitagawa, T.; Einaga, H. *Angew. Chem., Int. Ed. Engl.* **1998**, *37*, 798–799.
- (11) Takahashi, Y.; Hashimoto, M.; Hikichi, S.; Akita, M.; Moro-oka, Y. *Angew. Chem., Int. Ed. Engl.* **1999**, *38*, 3074–3077.
- (12) Carmona, D.; Lamata, M. P.; Ferrer, J.; Modrego, J.; Perales, M.; Lahoz, F. J.; Atencio, R.; Oro, L. A. *J. Chem. Soc., Chem. Commun.* **1994**, 575–576.
- (13) Thewalt, U.; Marsh, R. *J. Am. Chem. Soc.* **1967**, *89*, 6364–6365.

- (14) Le Carpentier, J.-M.; Mitschler, A.; Weiss, R. *Acta Crystallogr., Section B* **1972**, 1288–1298.
- (15) Akita, M.; Miyaji, T.; Hikichi, S.; Moro-oka, Y. *Chem. Lett.* **1999**, 813–814.
- (16) Wang, W.-D.; Bakac, A.; Espenson, J. H. *Inorg. Chem.* **1995**, *34*, 4049–4056.
- (17) Kumar, K.; Endicott, J. F. *Inorg. Chem.* **1984**, *23*, 2447–2452.
- (18) Geiger, T.; Anson, F. C. *J. Am. Chem. Soc.* **1981**, *103*, 7489–7496.

attention, mostly in the context of photochemically induced oxidation of organic materials. Evolution of oxygen is often observed,^{19–25} but the detailed mechanism(s) of such reactions have been investigated in only a few cases. The photolysis of an oxoperoxovanadium(V) complex, $\text{VO}(\text{O}_2)^+$, yields the hydroperoxyl radical, HO_2^* ,²⁶ which reacts with more $\text{VO}(\text{O}_2)^+$ and produces O_2 and H_2O_2 via an observable intermediate believed to be $\text{VO}(\text{O}_2)(\text{HO}_2)^+$. Peroxotitanium(IV) porphyrins have been reported to undergo cleavage of both $\text{O}-\text{O}$ ²⁷ and $\text{Ti}-\text{O}$ bonds.²¹ A peroxy superoxomolybdenum(V) complex was proposed as a short-lived intermediate in the photochemical cleavage of diperoxomolybdenum(VI) porphyrins to O_2 and peroxomolybdenum(IV).²⁰ The photolysis of a μ -peroxodicobalt(III) complex produces O_2 on a nanosecond time scale, suggesting that O_2 is a primary photoproduct.²² The complex $(\text{TPP})(\text{dmf})\text{Co}(\text{O}_2)^-$ (TPP = tetraphenylporphyrin, dmf = dimethylformamide) yields $(\text{TPP})(\text{dmf})\text{Co}$ and superoxide upon 355-nm photolysis in dmf.²⁸ In $\text{dmf}/\text{H}_2\text{O}$, where the peroxy complex was presumed to have been converted to the hydroperoxy form, $(\text{TPP})(\text{DMF})\text{CoOOH}$, the photoirradiation again yielded cobalt(II) and, presumably, HO_2^* .

In the present work we have investigated the visible and UV photochemistry of $\text{L}^2(\text{H}_2\text{O})\text{CoOOH}^{2+}$. Laser flash photolysis studies were carried out utilizing the second, third and fourth harmonic output of a Nd:YAG laser ($\lambda_{\text{exc}} = 532, 355, \text{ and } 266 \text{ nm}$).

Experimental Section

Solutions of the hydroperoxy complex $\text{L}^2(\text{H}_2\text{O})\text{CoOOH}^{2+}$ were prepared by $\text{Ru}(\text{NH}_3)_6^{2+}$ reduction of $\text{L}^2(\text{H}_2\text{O})\text{CoOO}^{2+}$, as previously described.¹⁶ The material was ion exchanged on Sephadex C-25 resin and eluted with 0.4 M $\text{CF}_3\text{SO}_3\text{Li}/0.05 \text{ M } \text{CF}_3\text{SO}_3\text{H}$. Small amounts of solid NaClO_4 were added to the purified solution which was then placed in a freezer. The solid material that precipitated after several days was redissolved in 1:1 $\text{H}_2\text{O}/\text{CH}_3\text{CN}$ and allowed to stand in a freezer. Yellow, needlelike crystals suitable for structure determination appeared after several days.

Caution: Perchlorate salts of metal complexes are potentially explosive and should be handled with care.

The crystal evaluation and data collection were performed on a Bruker CCD-1000 diffractometer with $\text{Mo K}\alpha$ ($\lambda = 0.71073 \text{ \AA}$) radiation. The final cell constants were calculated from a set of 4536 reflections. The systematic absences in the diffraction data were uniquely consistent for the space group $P2_1/n$ that yielded chemically reasonable and computationally stable results of refinement.²⁹ A successful solution by the direct methods provided most non-hydrogen atoms from the E-map. The remaining non-hydrogen atoms were located

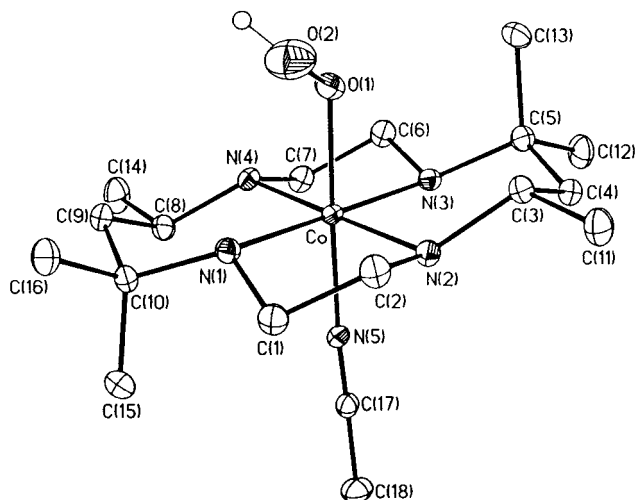


Figure 1. Perspective view of $\text{L}^2(\text{CH}_3\text{CN})\text{CoOOH}^{2+}$ with the thermal ellipsoids at the 30% probability level. Selected bond distances (\AA) and angles ($^\circ$): $\text{Co}-\text{O}(1)$ 1.878(3), $\text{Co}-\text{N}(1)$ 1.994(3), $\text{Co}-\text{N}(2)$ 1.997(3), $\text{Co}-\text{N}(3)$ 2.025(3), $\text{Co}-\text{N}(4)$ 1.978(3), $\text{Co}-\text{N}(5)$ 1.940(3), $\text{O}(1)-\text{O}(2)$ 1.397(4), $\text{O}(1)-\text{Co}-\text{N}(5)$ 176.30(12), $\text{O}(2)-\text{O}(1)-\text{Co}$ 117.7(2).

in an alternating series of least-squares cycles and difference Fourier maps. All non-hydrogen atoms were refined with anisotropic displacement coefficients. All hydrogen atoms were included in the structure factor calculation as idealized contributions. There is also one solvate molecule of acetonitrile present in the asymmetric unit. The absorption correction was based on fitting a function to the empirical transmission surface as sampled by multiple equivalent measurements.³⁰

Laser flash photolysis experiments utilized the second, third and fourth harmonic of a Nd:YAG laser which is a part of the Applied Photophysics instrument described earlier.³¹ All the flash photolysis experiments utilized acidic solutions of $\text{L}^2(\text{H}_2\text{O})\text{CoOOH}^{2+}$, because the complex decomposes at $\text{pH} > 4$.

The infrared spectra of $[\text{L}^2(\text{CH}_3\text{CN})\text{CoOOH}][\text{ClO}_4]_2 \cdot \text{CH}_3\text{CN}$ and $[\text{L}^2\text{Co}(\text{H}_2\text{O})_2](\text{CF}_3\text{SO}_3)_2$ were obtained by use of a Bio-Rad Digilab FTS-60A FT-IR spectrometer equipped with an MTEC Model 200 photoacoustic cell.³² Several milligrams of the solid material were placed into a small aluminum cup and inserted into the sample compartment. All of the material was recovered after the completion of data collection.

Results and Discussion

Crystal Structure of $[\text{L}^2(\text{CH}_3\text{CN})\text{CoOOH}][\text{ClO}_4]_2 \cdot \text{CH}_3\text{CN}$.

The molecular structure of the cation $\text{L}^2(\text{CH}_3\text{CN})\text{CoOOH}^{2+}$ is shown in Figure 1. The coordination about the cobalt is slightly distorted octahedral with four nitrogen atoms in the equatorial plane, and the acetonitrile and hydroperoxy ligands in the apical positions. The cobalt atom is essentially coplanar with the equatorial nitrogen atoms (within 0.010 (1) \AA). The average equatorial $\text{Co}-\text{N}$ bond length is 1.98 (2) \AA , and the axial $\text{Co}-\text{N}(5)$ bond length is 1.940(3) \AA . All the $\text{Co}-\text{N}$ distances are in good agreement with the corresponding bonds in other complexes of $\text{Co}(\text{Me}_6[14]\text{aneN}_4)$ and $\text{Co}(14\text{-aneN}_4)$.^{33–36} The

(19) Ledon, H.; Bonnet, M.; Lallemand, J. Y. *J. Chem. Soc., Chem. Commun.* **1979**, 702–704.

(20) Ledon, H. J.; Bonnet, M.; Galland, D. *J. Am. Chem. Soc.* **1981**, *103*, 6209–6211.

(21) Boreham, C. J.; Latour, J. M.; Marchon, J. C.; Boisselier-Cocolios, B.; Guilard, R. *Inorg. Chim. Acta* **1980**, *45*, 69–71.

(22) MacArthur, R.; Sucheta, A.; Chong, F. F. S.; Einarsson, O. *Proc. Natl. Acad. Sci. U.S.A.* **1995**, *92*, 8105–8109.

(23) Kikkawa, M.; Sasaki, Y.; Kawata, S.; Hatakeyama, Y.; Ueno, F. B.; Saito, K. *Inorg. Chem.* **1985**, *24*, 4096–4010.

(24) Munuera, G.; Gonzalez-Elipe, A. R.; Fernandez, A.; Malet, P.; Espinos, J. P. *J. Chem. Soc., Faraday Trans. 1* **1989**, *85*, 1279–1290.

(25) Shinohara, N.; Matsufuji, S.; Okubo, W. *Polyhedron* **1991**, *10*, 107–112.

(26) Shinohara, N.; Nakamura, Y. *Bull. Chem. Soc. Jpn.* **1989**, *62*, 734–737.

(27) Hoshino, M.; Yamamoto, K.; Lillis, J. P.; Chijimatsu, T.; Uzawa, J. *Inorg. Chem.* **1993**, *32*, 5002–5003.

(28) Hoshino, M.; Seki, H.; Yamaji, M.; Hama, Y. *Photochem. Photobiol.* **1993**, *57*, 728–731.

(29) All software and sources of the scattering factors are contained in the SHELXTL (version 5.1) program library (G. Sheldrick, Bruker Analytical X-ray Systems, Madison, WI).

(30) Blessing, R. H. *Acta Crystallogr.* **1995**, *A51*, 33–38.

(31) Huston, P.; Espenson, J. H.; Bakac, A. *J. Am. Chem. Soc.* **1992**, *114*, 9510–9516.

(32) Bajic, S. J.; Luo, S.; Jones, R. W.; McClelland, J. F. *Appl. Spectroscopy* **1995**, *49*, 1000–1003.

(33) Endicott, J. F.; Lilie, J.; Kuszaj, J. M.; Ramaswamy, B. S.; Schmonsees, W. G.; Simic, M. G.; Glick, M. D.; Rillema, D. P. *J. Am. Chem. Soc.* **1977**, *99*, 429–439.

(34) Bakac, A.; Espenson, J. H. *Inorg. Chem.* **1987**, *26*, 4353–4355.

(35) Bakac, A.; Espenson, J. H.; Young, V. G., Jr. *Inorg. Chem.* **1992**, *31*, 4959–4964.

(36) Knoch, F.; Thaler, F.; Schindler, S. *Z. Kristallogr.* **1996**, *211*, 717–718.

Table 1. Crystallographic Data for $[\text{L}^2(\text{CH}_3\text{CN})\text{CoOOH}](\text{ClO}_4)_2 \cdot \text{CH}_3\text{CN}$

chemical formula	$\text{C}_{20}\text{H}_{43}\text{Cl}_2\text{CoN}_6\text{O}_{10}$	$Z = 4$
formula wt	657.43	temp = 173(2) K
space group	$P21/n$	wavelength = 0.71073 Å
$a = 10.4230(5)$ Å		ρ (calcd) = 1.486 Mg/m ³
$b = 16.1561(8)$ Å		$\mu = 0.825$ mm ⁻¹
$c = 17.4676(9)$ Å		$R1 = 0.0534^a$
$\beta = 92.267(1)^\circ$		wR2 = 0.1373 ^b
$V = 2939.2(3)$ Å ³		

^a $R1 = \Sigma \Delta / \Sigma (F_0)$, $\Delta = |F_0 - F_c|$. ^b $R(wF2) = \Sigma [w(F_0^2 - F_c^2)] / \Sigma [w(F_0^2)]^{0.5}$.

Table 2. Hydrogen Bonds (Å) in $[\text{L}^2(\text{CH}_3\text{CN})\text{CoOOH}](\text{ClO}_4)_2 \cdot \text{CH}_3\text{CN}^a$

D—H···A	$d(\text{D—H})$	$d(\text{H···A})$	$d(\text{D···A})$	$\angle \text{DHA}$ (deg)
O(2)—H···O(10)	0.84	2.12	2.934(6)	164.2
N(1)—H···O(2)	0.93	2.00	2.732(5)	134.0
N(2)—H···O(6)	0.93	2.27	3.108(4)	149.1
N(3)—H···O(9)	0.93	2.27	3.180(4)	166.1
N(4)—H···O(3)	0.93	2.32	3.125(4)	144.9

^a D = donor, A = acceptor.

R,R,S,S stereochemistry around the nitrogens of the macrocyclic ligand is the same as that of the starting $\text{L}^2\text{Co}(\text{H}_2\text{O})_2^{2+}$.^{36–38}

To the best of our knowledge, the crystal structure of $\text{L}^2(\text{CH}_3\text{CN})\text{CoOOH}^{2+}$ is the first reported structure of a mononuclear hydroperoxo cobalt complex. The OOH group is bound in the end-on fashion, the Co—O—O angle is 117.7(2)°, and the O—O bond length is 1.397(4) Å, similar to those in other known hydroperoxo complexes.^{9–12,39,40}

Five types of hydrogen bonds in the structure form a three-dimensional network in the lattice. The hydrogen bonds vary in type and strength as shown in Table 2. The hydroperoxo group is involved in intramolecular hydrogen bonding with an N—H group, and intermolecular hydrogen bonding with a perchlorate ion. The three remaining N—H groups are all hydrogen bonded to perchlorate ions.

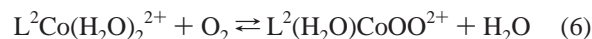
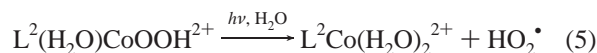
IR Spectra. A part of the infrared spectra of $[\text{L}^2\text{Co}(\text{H}_2\text{O})_2](\text{CF}_3\text{SO}_3)_2$ (a) and $[\text{L}^2(\text{CH}_3\text{CN})\text{CoOOH}](\text{ClO}_4)_2 \cdot \text{CH}_3\text{CN}$ (b) is shown in Figure S1 (Supporting Information). The two spectra have identical features except for two extra peaks, one at 760 cm⁻¹ in (a) and one at 815 cm⁻¹ in (b). We assign the 760 cm⁻¹ band to a C—F stretch in the triflate anion and the 815 cm⁻¹ band to the O—O stretch in the hydroperoxide. The frequency of the O—O stretch is in the expected range (800–900 cm⁻¹) for a coordinated (hydro)peroxo group.^{5,10,12,41–46}

Laser Flash Photolysis. No absorbance change was observed at $\lambda > 260$ nm when an argon-saturated aqueous solution of 0.3 mM $\text{L}^2(\text{H}_2\text{O})\text{CoOOH}^{2+}$ in 0.01 M HClO_4 was irradiated in a 532 nm laser flash. When the irradiating wavelength was changed to 355 nm, a bleach in absorbance was observed

throughout the UV range. To test for the possible formation of HO^\bullet radicals, an experiment was conducted in the presence of 1 M 2-propanol and 0.5 mM methyl viologen, MV^{2+} . No absorbance increase was observed at 600 nm where MV^{2+} exhibits an absorption maximum, $\epsilon = 1.37 \times 10^4 \text{ M}^{-1} \text{ cm}^{-1}$.⁴⁷ This result rules out the formation of HO^\bullet which would have led to the generation of MV^{+} as shown in eqs 3 and 4.^{48,49}



When the photolysis of $\text{L}^2(\text{H}_2\text{O})\text{CoOOH}^{2+}$ (0.2 mM) in 0.01 M HClO_4 was carried out in oxygen-saturated solutions, the absorbance at 360 nm decreased in the flash and then increased exponentially to slightly above the pre-flash value with $k = 2.4 \times 10^4 \text{ s}^{-1}$. This rate constant agrees well with the kinetics of the $\text{L}^2\text{Co}(\text{H}_2\text{O})_2^{2+} - \text{O}_2$ reaction, for which we calculate a rate constant of $2.6 \times 10^4 \text{ s}^{-1}$ under these reaction conditions.³⁸ This result suggests that the photochemistry takes place as in eq 5, followed by the known³⁸ equilibration reaction of eq 6.



The other photolysis product, $\text{HO}_2^\bullet/\text{O}_2^{\bullet-}$, was detected with tetranitromethane, which is reduced rapidly⁵⁰ by $\text{O}_2^{\bullet-}$ to produce nitroform anion, $\text{C}(\text{NO}_2)_3^-$, $\lambda_{\text{max}} 350 \text{ nm}$, $\epsilon = 1.5 \times 10^4 \text{ M}^{-1} \text{ cm}^{-1}$, eq 7.



The reaction was carried out at two different concentrations of H^+ , 1.0 mM and 3.0 mM. In both cases, the absorbance at 350 nm increased exponentially after the flash. The plots of k_{obs} against the concentration of TNM were linear, Figure S2 (Supporting Information), yielding $k = 4.37 \times 10^7 \text{ M}^{-1} \text{ s}^{-1}$ at 1.0 mM H^+ and $1.46 \times 10^7 \text{ M}^{-1} \text{ s}^{-1}$ at 3.0 mM H^+ . Taking $K_a = 1.6 \times 10^{-5} \text{ M}$ for $\text{HO}_2^\bullet/\text{O}_2^{\bullet-}$,⁵⁰ the two values yield $k_7 = 2.8 \times 10^9 \text{ M}^{-1} \text{ s}^{-1}$ for the reaction of $\text{O}_2^{\bullet-}$ with TNM, in reasonable agreement with the reported⁵⁰ value of $2.0 (\pm 0.4) \times 10^9 \text{ M}^{-1} \text{ s}^{-1}$. The detection of both $\text{L}^2\text{Co}(\text{H}_2\text{O})_2^{2+}$ and $\text{HO}_2^\bullet/\text{O}_2^{\bullet-}$ clearly establishes that the 355-nm photolysis of $\text{L}^2(\text{H}_2\text{O})\text{CoOOH}^{2+}$ takes place by homolytic cleavage of the Co—O bond as shown in eq 5.

For equimolar yields of $\text{L}^2\text{Co}(\text{H}_2\text{O})_2^{2+}$ and $\text{HO}_2^\bullet/\text{O}_2^{\bullet-}$ in eq 5, the absorbance change in reaction 7 should be ~10 times greater than that in reaction 6. The observed ratio was somewhat smaller, ~5, probably as a result of the known⁵¹ secondary reaction between NO_2 and HO_2^\bullet which diminishes the amount of $\text{O}_2^{\bullet-}$ available for the reaction with $\text{C}(\text{NO}_2)_4$. Also, to improve the signal-to-noise ratio in eq 6, several traces were accumulated and averaged. In the later shots, however, the reversible photochemistry of the product $\text{L}^2(\text{H}_2\text{O})\text{CoOO}^{2+}$ contributes and artificially increases the overall absorbance change.

- (37) Rillema, P.; Endicott, J. F.; Papaconstantinou, E. *Inorg. Chem.* **1971**, *10*, 1739–1746.
 (38) Bakac, A.; Espenson, J. H. *J. Am. Chem. Soc.* **1990**, *112*, 2273–2278.
 (39) Vaska, L. *Acc. Chem. Res.* **1976**, *9*, 175–183.
 (40) Jones, R. D.; Summerville, D. A.; Basolo, F. *Chem. Rev.* **1979**, *79*, 139–179.
 (41) Nakamoto, K. *Coord. Chem. Rev.* **1990**, *100*, 363–402.
 (42) Morvillo, A.; Bressan, M. *J. Organomet. Chem.* **1987**, *332*, 337–343.
 (43) Root, D. E.; Mahroof-Tahir, M.; Karlin, K. D.; Solomon, E. I. *Inorg. Chem.* **1998**, *37*, 4838–4848.
 (44) Suzuki, H.; Matsuura, S.; Moro-oka, Y.; Ikawa, T. *J. Organomet. Chem.* **1985**, *286*, 247–258.
 (45) Roberts, H. L.; Symes, W. R. *J. Chem. Soc. A* **1968**, 1450–1453.
 (46) Strukul, G.; Ros, R.; Michelin, R. A. *Inorg. Chem.* **1982**, *21*, 495–500.

- (47) Watanabe, T.; Honda, K. *J. Phys. Chem.* **1982**, *86*, 2617–2619.
 (48) Buxton, G. V.; Greenstock, C. L.; Helman, W. P.; Ross, A. B. *J. Phys. Chem. Ref. Data* **1988**, *17*, 513–886.
 (49) Venturi, M.; Mulazzani, Q. G.; Ciano, M.; Hoffman, M. Z. *Inorg. Chem.* **1986**, *25*, 4493–4498.
 (50) Bielski, B. H. J.; Cabelli, D. E.; Arudi, R. L.; Ross, A. B. *J. Phys. Chem. Ref. Data* **1985**, *14*, 1041–1100.
 (51) Sutton, H. C. *J. Chem. Soc., Faraday Trans. 1* **1975**, *71*, 2142–2147.

The 266-nm flash photolysis also produced $L^2Co(H_2O)_2^{2+}$ and $HO_2^*/O_2^{\bullet-}$, as shown by their reactions with O_2 and TNM, respectively. The initial concentration of $L^2(H_2O)CoOOH^{2+}$ had to be kept low (0.03 mM) because of its large molar absorptivity at this wavelength ($\epsilon_{266} \sim 7000 \text{ M}^{-1} \text{ cm}^{-1}$).¹⁶ The photolysis yields and the signal-to-noise ratio were quite low in these experiments, but the overall behavior of the system was qualitatively the same as that observed with $\lambda_{\text{irr}} = 355 \text{ nm}$. The rate constant for the $L^2Co(H_2O)_2^{2+}/O_2$ reaction was $(3.1 \pm 0.4) \times 10^4 \text{ s}^{-1}$ for $\lambda_{\text{irr}} = 266 \text{ nm}$.

The reaction between $HO_2^*/O_2^{\bullet-}$ and TNM, using $\lambda_{\text{irr}} = 266 \text{ nm}$, was studied at 0.67 mM H^+ . The kinetic traces showed a sudden absorbance increase during the flash, caused by direct photochemistry of TNM, followed by a slower increase after the flash. The kinetics of the latter stage gave $k = 2.8 \times 10^7 \text{ M}^{-1} \text{ s}^{-1}$. After correcting for the unreactive HO_2^* form, we obtain $k_7 = 1.2 (\pm 0.2) \times 10^9 \text{ M}^{-1} \text{ s}^{-1}$. The value is somewhat low, possibly indicating that the photochemistry of TNM affects the outcome. These possible complications aside, $C(NO_2)_3^-$ is clearly produced by 266-nm photolysis. Taken together, the results with O_2 and TNM show that the photochemistry of $L^2(H_2O)CoOOH^{2+}$ at 266 nm also takes place as in eq 5.

To check for a possible contribution from the homolytic O–O bond cleavage for $\lambda_{\text{irr}} = 266 \text{ nm}$, an experiment was carried out in 0.01 M HClO_4 under argon in the presence of $0.020 \text{ mM ABTS}^{2-}$ (2,2'-azinobis(3-ethylbenzothiazoline-6-sulfonate)). At this concentration, $ABTS^{2-}$ absorbs <0.3 at 266 nm, still allowing the desired photolysis of $L^2(H_2O)CoOOH^{2+}$ to take place to the extent of $>50\%$ of that observed in the absence of $ABTS^{2-}$. Any HO^* radicals produced would rapidly oxidize $ABTS^{2-}$ to $ABTS^{\bullet-}$ ($k = 1.2 \times 10^{10} \text{ M}^{-1} \text{ s}^{-1}$)⁴⁸ causing an increase in absorbance at 417 nm ($\epsilon_{ABTS^{\bullet-}} = 3.47 \times 10^4 \text{ M}^{-1} \text{ cm}^{-1}$).⁵² A small absorbance increase at 417 nm (corresponding to $0.2 \mu\text{M ABTS}^{\bullet-}$) was observed, but it was caused by the photochemistry of $ABTS^{2-}$ itself. This absorbance change and its rate were independent of the concentration of $L^2(H_2O)$ -

$CoOOH^{2+}$ and were observed even when no hydroperoxo complex was present.

Clearly, reaction 2c is unimportant for $L^2(H_2O)CoOOH^{2+}$, despite the dominance of this pathway for H_2O_2 and ROOH. This surprising finding is probably caused by the spectral characteristics of $L^2(H_2O)CoOOH^{2+}$. The intense maximum at 240 nm ($\epsilon = 1.4 \times 10^4 \text{ M}^{-1} \text{ cm}^{-1}$)¹⁶ is apparently caused by the HO_2 -to-Co ligand-to-metal charge transfer (LMCT) transition. This band tails out to close to 400 nm and thus dominates the spectrum and controls the photochemistry. Any absorbance associated with the O–O bond would be too weak in comparison with the LMCT band, resulting in very inefficient photochemistry of the peroxo bond. As a result, $L^2(H_2O)CoOOH^{2+}$ behaves similarly to the superoxo ($L^2(H_2O)CoOO^{2+}$) and alkyl ($L^2(H_2O)CoR^{2+}$) derivatives, both of which undergo photochemical homolysis of the respective Co–O and Co–C bonds.³⁸ Homolytic cleavage of the Co–O bond has also been observed for (TPP)(dmf)Co(O_2)⁻ and (presumably) (TPP)(dmf)Co(O_2 H).²⁸ We are currently exploring the use of $L^2(H_2O)CoOOH^{2+}$ and related hydroperoxo complexes as photochemical sources of $HO_2^*/O_2^{\bullet-}$ for kinetic and mechanistic studies.

Acknowledgment. This work was supported by the U.S. Department of Energy, Office of Basic Energy Sciences, Division of Chemical Sciences, under Contract No. W-7405-Eng-82. We are grateful to Dr. Stan Bajic for his help in obtaining the infrared spectra.

Supporting Information Available: Figures S1 and S2, crystallographic data in a CIF file, crystallographic tables, and an ORTEP including perchlorate anions (Figure S3). This material is available free of charge via the Internet at <http://pubs.acs.org>.

IC001391L

(52) Scott, S. L.; Chen, W.-J.; Bakac, A.; Espenson, J. H. *J. Phys. Chem.* **1993**, *97*, 6710–6714.